# Multilayer SPR hydrogen sensor based on a heterogeneous metal nanolayer

B. Aliche*, A. Saouli
*Microsystems and Instrumentation Laboratories (LMI), Faculty of Technology Sciences, Mentouri Brothers University of Constantine, Constantine, Algeria*

In this study, we created a multilayer SPR hydrogen sensor that is primarily based on an Ag-nd or Au-nd heterogeneous metal nanolayer. To characterize the response of the suggested structure, we used the Matlab program and the transfer matrix method (T-Matrix) in this investigation. We developed a set of sensors (n1/Ag-nd/Pd Or n1/Au-nd/Pd) with varying densities of metal nanoparticles N = 400[1/μm$^3$], 600[1/μm$^3$], 800[1/μm$^3$], and 1000 [1/μm$^3$], respectively, to verify the sensor's performance. They are assessed using a number of conventional standards, including sensitivity and minimum reflectance (Rmin). The sensor with Ag-nd layer and N = 1000 [1/μm$^3$] was found to attain the lowest Rmin of 0.04 and the highest sensitivity of S = 7.99[nm] with a maximum resonance wavelength shift of 2.4 [nm]. The suggested SPR hydrogen sensor may detect changes in palladium (Pd)'s optical characteristics and, consequently, leaks of hydrogen gas, according to simulation data.

(Received February 11, 2024; Accepted May 10, 2024)

*Keywords:* Multilayer SPR hydrogen sensor, Heterogeneous metal nanolayer, Sensitivity, T-Matrix

## 1. Introduction

One of the most promising energy sources available to us today is hydrogen [1]. This is because it is the most abundant, cleanest, most efficient, and renewable source. Its only byproduct is water, and it is also regarded as one of the lightest chemical elements. One of the most significant frequently utilized and helpful gasses is hydrogen gas. It is significant in a number of domains. Including the medical industry, where it powers various medical systems' electricity and heat generators to run labs and other medical equipment. It is also frequently employed in novel medical procedures [2]. Even though it seems harmless, the risks it poses to human life—namely, its propensity to ignite easily and burn for an extended period of time—make its storage and transportation an enormous challenge. An explosive and highly flammable atmosphere is created when hydrogen leaks and its concentration in the air surpasses 4%, also referred to as the lower explosive limit (LEL) [4–3]. Breathing hydrogen in excessive quantities can have detrimental effects on one's health. Thus, it's critical to intensify efforts to create sensing technologies that work. Inexpensive, dependable, and quick in identifying hydrogen leaks early on.

Numerous hydrogen sensors, including electrical [6–5] and optical [7-8] ones, have been discovered in recent years. Because optical sensors don't produce sparks and are electrically insulated, they were given special attention. These include sensors based on nanotechnology [9], surface plasmon resonance [11–12], and optical fibers [10–12] for hydrogen optical detection. The majority of them attempted to improve the sensor's sensitivity and response. Some people have strong sensitivity and achieve good results, whereas others have low sensitivity. The majority of these sensors were primarily dependent on thin-film palladium (Pd). Palladium (Pd) exhibits a remarkable capacity for hydrogen absorption; it may absorb up to 900 times its volume [13]. This leads to the formation of reversible palladium(PdHx) hydride. Palladium (Pd) metal interacts with hydrogen ($H_2$) as a result of all of this, changing its optical characteristics [14].

* Corresponding author: bouchra.aliche@doc.umc.edu.dz
https://doi.org/10.15251/DJNB.2024.192.731

Recently, surface plasmon resonance has been developed for use in detecting small changes in optical properties. It has been used to detect changes in the optical properties [15-16] of palladium metal when it interacts with hydrogen gas.

Surface plasmon resonance is a new technique that can be used to identify minute variations in optical characteristics. It has been applied to the detection of changes in the optical characteristics of palladium metal in response to hydrogen gas interactions [15–16]. In order to detect hydrogen, D. Sil et al. employed gold nanoparticles and palladium for the first time [17]. When exposed to hydrogen, the SPR wavelength changed by 3[nm] in just one second. An SPR hydrogen sensor from heterogeneous optical fibers using Au/Ta2O5/Pd/Au multilayers was reported by Ken Takahashi et al. in 2016. The sensor had a wavelength shift of 24.4 [nm] for the Pd-Au layer and 14.4 [nm] for the Au layer. Palladium shells and gold metal nanorods were used by R. Jiang et al. to produce remarkable sensitivity for the Pd layer at 4% hydrogen concentration [18, 19].

In the area of multilayer SPR detectors, we have several works, such as one that enhances the sensitivity of the detectors' spectrum response [20, 21] and another that theoretically investigates the double resonance SPR as the basis for angular interrogation [22]. This work presents a multilayer hydrogen surface plasmon resonance (SPR) sensor supported by a layer of palladium and a heterogeneous Ag-nd or Au-nd metal nanolayer. This sensor is based on how the interaction of palladium metal with hydrogen gas alters the metal's visual characteristics. Using the transfer matrices (T-matrix) method, we simulate the performance of a hydrogen SPR sensor. SPR resonance curves were constructed with variations in the resonance wavelength for various hydrogen concentrations. An analysis is conducted and the sensitivity is modified for optimal performance. To improve sensitivity, the impact of nanoparticle density on the heterogeneous metal nanolayer is examined.

## 2. Design theories and mathematical approach

The proposed SPR hydrogen sensor consists of three different layers. The first layer is an dielectric with a refractive index of n1, the second layer is a heterogeneous metallic nano layer with a refractive index of $n_{eff}$, and the third layer is palladium metal (Pd) with a refractive index of n2 , as shown in Fig1. the z-axis extends from medium 1 to medium 3, and the x-axis runs along the 1–2 interface.

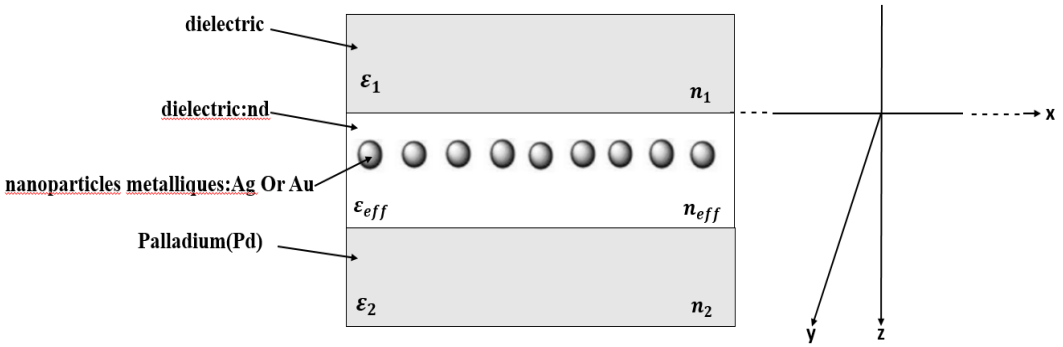


*Fig. 1. SPR hydrogen sensor structure based on a heterogeneous metallic nanolayer.*

A surface plasmon resonance is a polarized (TM) electromagnetic (EM) light wave propagating along the X- axis with the optical wave vector Kx and a refraction index $n_1$ and a certain angle of incidence θn and with the Longitudinal propagation vector Kz according to the following equations respectively[23-24-25-26 ]:

$$k_{x=}\mathrm{k}_0 n_1 sin(\theta_n) \quad (1)$$

where $k_0 = \frac{w}{c}$ represents the propagation vector of light in a vacuum.

$$k_{z1} = \sqrt{\left(n_1 \frac{w}{c}\right)^2 - kx^2} \quad (2)$$

$$k_{z2} = \sqrt{\left(n_{eff} \frac{w}{c}\right)^2 - kx^2} \quad (3)$$

$$k_{z3} = \sqrt{\left(n_2 \frac{w}{c}\right)^2 - kx^2} \quad (4)$$

In our simulations, we depend on the transfer matrix method in order to calculate the optical response of the proposed multilayered structure.

We have an interface scattering matrix that describes the transmission of fields between two adjacent layers and they are called i and j [27]:

$$H_{ij} = \frac{1}{\tau_{ij}} \begin{pmatrix} 1 & \rho_{ij} \\ \rho_{ij} & 1 \end{pmatrix} \quad (5)$$

We also have the scattering matrix of layer j [25]:

$$L_j = \begin{pmatrix} e^{j\beta} & 0 \\ 0 & e^{j\beta} \end{pmatrix} \quad (6)$$

where

$$\beta = \frac{2\pi}{\lambda} dn \cos(\theta) \quad (7)$$

By combining the two matrices H and L we get the matrix S which is the diffusion matrix that characterizes the optical response of the multilayered structure j [29]:

$$S = L_{01}\, H_1\, L_{12} H_2 \ldots\ldots\ldots H_N L_{N(N-1)} \quad (8)$$

$$S_{1N} = \begin{pmatrix} S_{11} & S_{12} \\ S_{21} & S_{22} \end{pmatrix} \quad (9)$$

In the end, we obtain the results of the reflectance coefficient of the multilayer structure given by the following relation:

$$R = \frac{S_{21}}{S_{11}} \quad (10)$$

The metals used in this study are gold and silver with thicknesses of dAu and dAg respectively, and in order to calculate the dielectric constant for Au and Ag we relied on a model of Drude with two critical points (D2CP) which is characterized by [30]:

$$\epsilon_{D2CP} = \epsilon_\infty - \frac{w_D^2}{w^2 + i\gamma w} + \sum_{p=1}^{2} G_p(w) \quad (11)$$

With

$$G_p(w) = A_p\, \Omega_p \left(\frac{e^{i\emptyset p}}{\Omega_p - w - i\Gamma P} + \frac{e^{-i\emptyset p}}{\Omega_p + w + i\Gamma P}\right) \quad (12)$$

*Table 1. Optimized D2CP model parameters used to calculate the dielectric function of gold and silver in the wavelength range 400-1000 nm [30].*

| | **Gold** | **Silver** |
|---|---|---|
| $\epsilon_\infty$ | 1.0300 | 3.7325 |
| $w_D$**(rad.s$^{-1}$)** | $1.3064\times10^{16}$ | $1.3354\times10^{16}$ |
| $\gamma$ **rad.s$^{-1}$** | $1.1274\times10^{14}$ | $9.6875\times10^{13}$ |
| $A_1$ | 0.86822 | 2.0297 |
| $\Omega_1$ **(rad.s$^{-1}$)** | $4.0812\times10^{15}$ | $4.5932\times10^{17}$ |
| $\emptyset$**1 (rad)** | -0.60756 | -0.70952 |
| **Γ1 (rad.s$^{-1}$)** | $7.3277\times10^{14}$ | $1.0524\times10^{18}$ |
| $A_2$ | 1.3700 | -2.8925 |
| $\Omega_2$ **(rad.s$^{-1}$)** | $6.4269\times10^{15}$ | $4.7711\times10^{16}$ |
| $\emptyset$**2 (rad)** | -0.087341 | -1.4459 |
| **Γ2 (rad.s$^{-1}$)** | $6.7371\times10^{14}$ | $3.0719\times10^{15}$ |

In order to calculate the dielectric function of the heterogeneous medium, we have relied on Maxwell–Garnett equations [31-32] (equation 13):

$$\varepsilon_{eff} = \varepsilon_2 \frac{\varepsilon_1 + 2\varepsilon_2 + 2f(\varepsilon_1 - \varepsilon_2)}{\varepsilon_1 + 2\varepsilon_2 - f(\varepsilon_1 - \varepsilon_2)} \tag{13}$$

where
f = N × V is the volume fraction occupied by the nanoparticles.

To realize the proposed multi-layered hydrogen SPR sensor with a heterogeneous metal nanolayer, we used as mentioned above Pd as the $H_2$ sensing layer, which is characterized by its optical properties when interacting with hydrogen gas **(**$H_2$**)**. The effects of hydrogen gas absorption on the complex dielectric function of palladium can be expressed by the following equation [33]:

$$\varepsilon_{Pd,c\%2H_2} = h(c\%) \times \varepsilon_{Pd,c\%H_2} \tag{14}$$

where $\varepsilon_{Pd,0\%H2}$ is the dielectric complex permittivity of palladium(Pd) in the absence of concentration **(**$H_2$**)**, h(c%) it is a nonlinear function that decreases with increasing hydrogen concentration Its values are less than1. In previous studies [34-35], the Drude-Lorentz (DL) model was used to calculate the permittivity of palladium(Pd) according to the following equation:

$$\varepsilon = \varepsilon_{hf} - \frac{1}{\Omega}\left(\frac{\Omega^2 pe}{\Omega + i\gamma_{oe}} + \frac{\Omega^2 ph}{\Omega + i\gamma_{oh}}\right) + \frac{1}{z}\sum_{j=1}^{k} \frac{f_j\, \Omega^2 pe}{\Omega^2 j - \Omega^2 - i\Omega_{\gamma j}} \tag{15}$$

## 3. Results and discussion

We modelled how the suggested structure might behave in the visible and near-infrared spectrums. Using a heterogeneous metal nanolayer comprising Ag-nd (a) and Au-nd (b) with a thickness of 50 [nm] and a metal nanoparticle density of 800[1/μm3] with varying hydrogen concentrations, Fig. 2 displays SPR curves as a function of wavelength. They rise as h values decrease, and are represented by the numbers 1, 0.9, 0.8, and 0.7, with h(1) = 0% and h(0.8) = 4% [36].

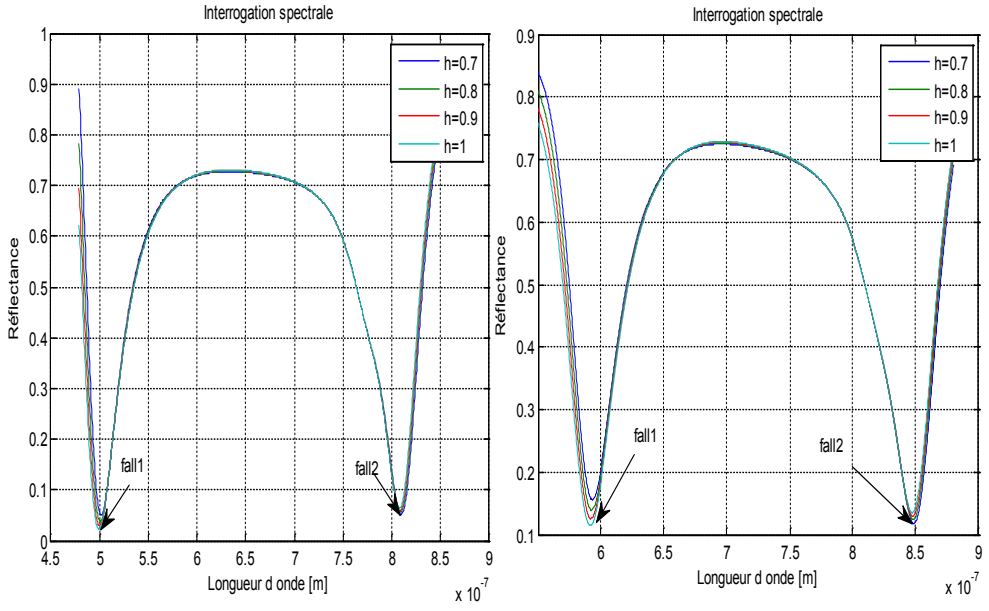


*(a)* *(b)*

*Fig. 2. SPR curves as a function of wavelength of the hydrogen sensor with different values of the parameter h: n1 = 2.58, Theta = π / 5 [rad], N = 800[1/μm3]; a) With a heterogeneous layer of metal nanoparticles Ag-nd ;b) With a heterogeneous layer of metal nanoparticles Au-nd.*

It was discovered that there are two distinct falls in which the SPR effect manifests itself. The first fall is caused by Ag (Fig. 2(a) and Au (Fig. 2(b) metals, whereas the second fall is caused by palladium (Pd) metal. Furthermore, in the visible and near-infrared spectrum, the double SPR effect is plainly visible.

The second fall's reflectance spectra with a heterogeneous metal nanolayer for Ag-nd (a) and Au-nd (b) at various hydrogen concentrations within the previously published range are displayed in Fig. 3 as a function of wavelength. We note a shift in the resonance wavelength from 804.2[nm] to 806.2[nm] was observed with an increase in the minimum of reflectance for each resonance wavelength when hydrogen gas flowed at standard concentrations within the previously reported range.

This is depicted in Fig. 3(a), along with a slight change in the minimum reflectance from 0.10 to 0.08, which is a value very close to zero, making it suitable to ensure the design of a high-performance sensor with good response and higher accuracy [37]. We can see in Fig. 3(b) that when the concentration of hydrogen rises, the resonance wavelength increases, with an alteration from 844.6[nm] to 846.2[nm]. Additionally, we note that the minimum reflectance has changed from 0.16 to 0.14. These modifications all point to the ability of the suggested hydrogen SPR sensor to identify variations in the optical characteristics of the palladium (Pd) that results from the absorption of hydrogen gas.

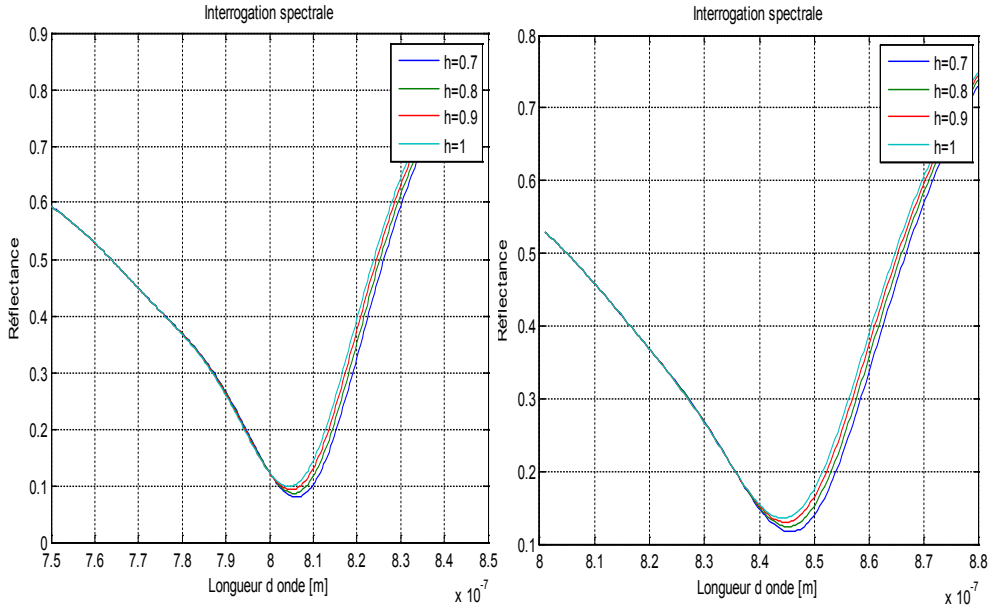


*Fig. 3. Variation of the reflectance spectra of the SPR hydrogen sensor for fall2 with different values of the parameter h : n1 = 2.58, Theta = π / 5 [rad], N = 800[1/µm3] ; a) With a heterogeneous layer of metal nanoparticles Ag-nd ;b) With a heterogeneous layer of metal nanoparticles Au-nd.*

We found a relationship between the change in the resonance wavelength and the hydrogen concentration that increases with the lowering of the variable h in order to ensure hydrogen gas detection and the accuracy of our sensor performance. This phase of the investigation involved comparing the performance of the suggested SPR sensor for various metal nanoparticle densities, where N is equivalent to 400 [1/µm$^3$], 600 [1/µm$^3$], 800 [1/µm$^3$], and 1000 [1/µm$^3$] for a heterogeneous metal nanolayer of Ag-nd and Au-nd, respectively, as illustrated in Figs 4 and 5, respectively.

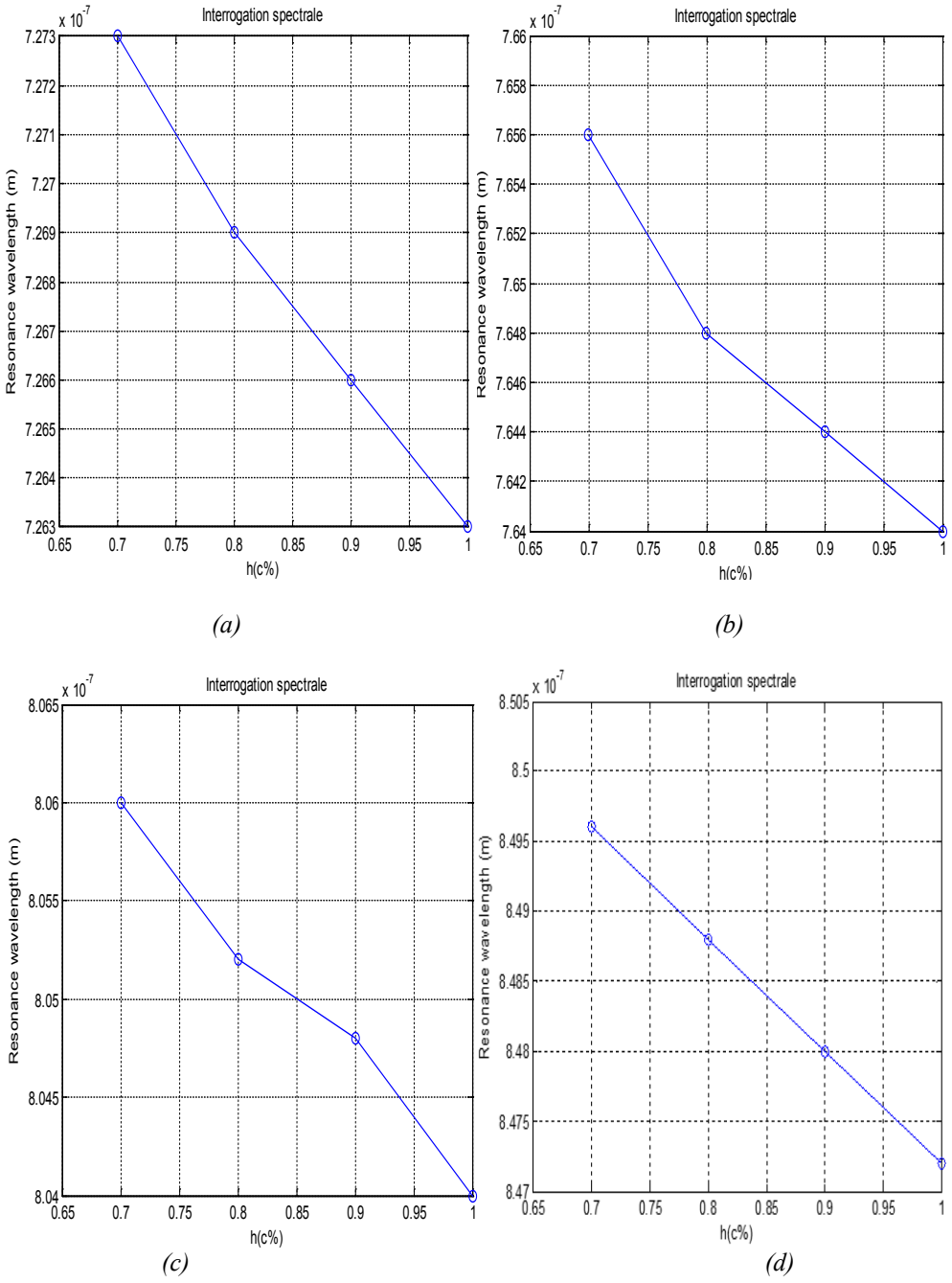


*Fig. 4.. Resonance wavelength shifts as a function of h; a) N=400[1/μm3] ; b) N=600 [1/μm3] ; c) N= 800 [1/μm3] ;d) N= 1000 [1/μm3] , n1 = 2.58, Theta = π / 5 [rad], tAg-nd =50 [nm].*

Using the optical and geometrical parameters provided in Figs. 4(a,b,c,d) and 5(a,b,c,d), it is demonstrated from the obtained results that the sensor has good linearity by the resonance wavelength shifts by varying the hydrogen concentration near the lower explosive limit (LEL). Additionally, it was discovered that the SPR hydrogen sensor configuration with the metal nanoparticle density N equal to 1000 [1/μm$^3$] exhibits a quasi-linear combination with the parameters shown in Figs 4(d) and 5(d), respectively. As the concentration of hydrogen rises, the Ag-nd layer's SPR resonance wavelength shifts by 1 [nm], 1.6 [nm], 2 [nm], and 2.4 [nm] at N equal to 400 [1/μm$^3$], 600 [1/μm$^3$], 800 [1/μm$^3$], and 1000 [1/μm$^3$], in that order, as illustrated in Fig 4. Regarding the Au-nd layer, Fig. 5 illustrates the changes in the SPR resonance wavelength that occur at N equal to 400 [1/μm$^3$], 600 [1/μm$^3$], 800 [1/μm$^3$], and 1000 [1/μm$^3$], respectively: 0.8[nm], 1.2[nm], 1.6 [nm], and 1.8 [nm]. These findings demonstrate that the SPR hydrogen

sensor with Ag-nd layer had superior optical changes compared to the SPR hydrogen sensor with Au-nd layer.

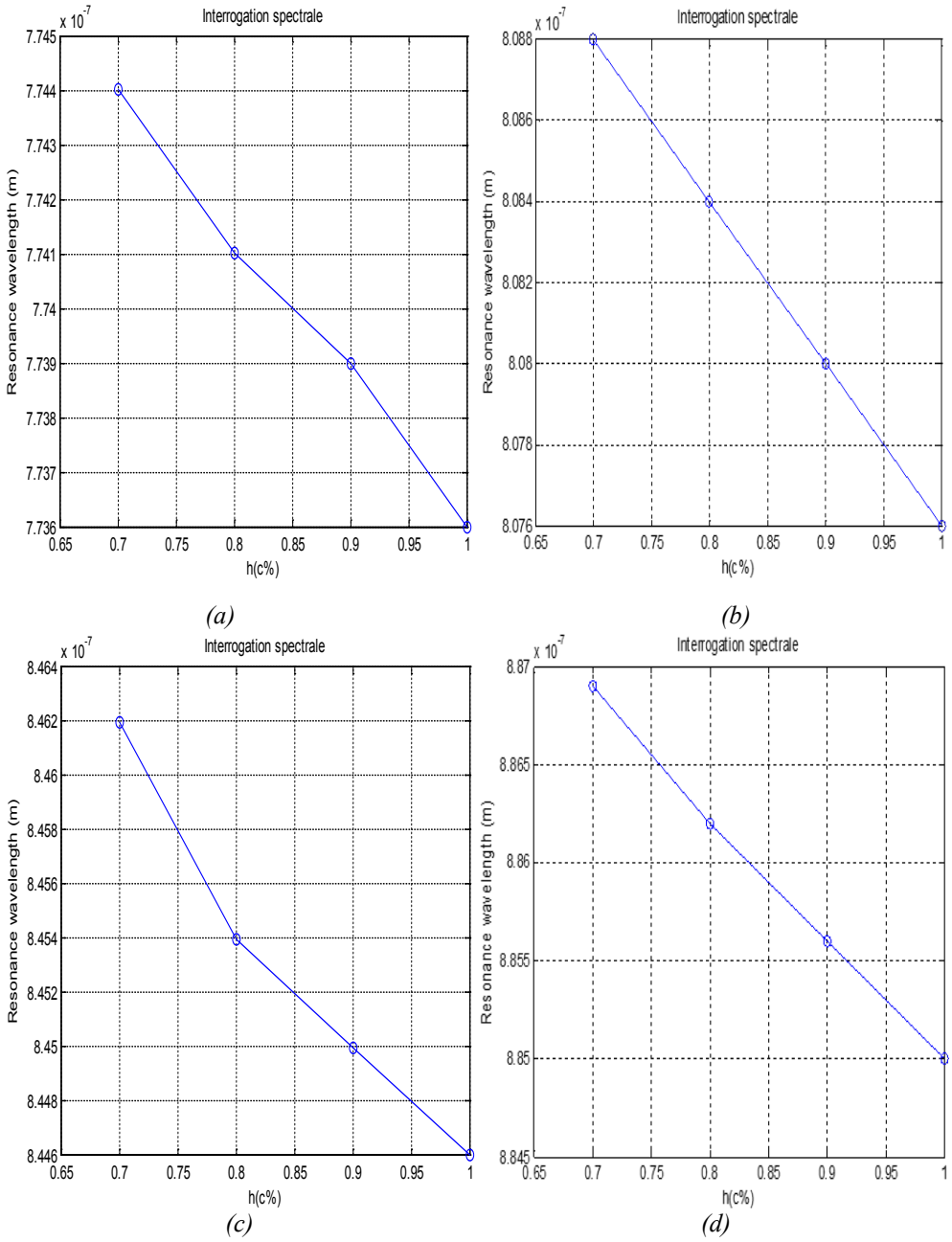


*Fig. 5. Resonance wavelength shifts as a function of h; a) N=400[1/μm3] ; b) N=600 [1/μm3] ; c) N= 800 [1/μm3] ; d) N= 1000 [1/μm3] n1 = 2.58, Theta = π / 5 [rad], tAu-nd =50 [nm].*

Using N equal to 400[1/μm$^3$], 600[1/μm$^3$], 800[1/μm$^3$], and 1000[1/μm$^3$], we compute the minimum reflectance Rmin of the Ag-nd and Au-nd multilayer SPR hydrogen sensor in the next inspection step. Table 1 displays the performance metrics that were determined for each of the suggested configurations; furthermore, we computed the sensor's sensitivity by examining changes in the hydrogen concentration ratio and the curve's resonance wavelength. The following formula can be used to indicate reflection:

$$S = \frac{\Delta\lambda_{res}}{\Delta h_{(c\%)}} \tag{16}$$

*Table 2. Performance parameters of the proposed multilayer SPR hydrogen sensor with a heterogeneous metal nanolayer such as:Ag-nd, Au-nd.*

**Ag-nd**

| **Density of metallic nanoparticles[1/μm$^3$]** | **400** | **600** | **800** | **1000** |
|---|---|---|---|---|
| **Rmin** | 0.20 | 0.13 | 0.08 | 0.04 |
| **Sensitivity [nm]** | 3.33 | 5.33 | 6.66 | 7.99 |

**Au-nd**

| **Density of metallic nanoparticles[1/μm$^3$]** | **400** | **600** | **800** | **1000** |
|---|---|---|---|---|
| **Rmin** | 0.25 | 0.20 | 0.14 | 0.11 |
| **Sensitivity [nm]** | 2.66 | 3.99 | 5.33 | 6.33 |

It is shown that the minimum reflectance, or Rmin, falls and the sensitivity increases with an increase in metal nanoparticle density. As it guarantees the link between the surface plasmon and the maximum energy of polarized light (TM), bringing Rmin close to zero is essential to increase the sensitivity and accuracy of the sensor [37]. The Ag-nd layer's highest sensitivity is observed at N = 1000[1/μm$^3$], when S = 7.99 [nm] and Rmin drop to 0.04. Regarding the Au-nd layer, we discover that the maximal sensitivity attained at N is equivalent to 1000[1/μm$^3$], S=6.33[nm], and Rmin drops to 0.11.The suggested sensor with Ag-nd heterogeneous metal nanoparticles and N equal to 1000[1/μm$^3$] will be the best option for detecting hydrogen gas leakage, based on the findings we were able to get.

## 4. Conclusion

We presented a multilayer SPR hydrogen sensor with an Ag-nd and Au-nd heterogeneous metal nanolayer in our current study. This work is based on the visible and near-infrared structural response. The resonance wavelength of the sensor increased for the Ag-nd and Au-nd layers, and was displaced by 2.4 and 1.6 nm, respectively, when it was subjected to standard amounts of hydrogen gas. Furthermore, it was discovered that the density of the metal nanoparticles and the kind of metal utilized in the construction had an impact on the sensitivity. Since it has the lowest Rmin value and the highest sensitivity, the sensor with Ag-nd layer and N equal to 1000 is a good option for detection. Ultimately, the simulation results demonstrated that the highest sensitivity of the multilayer hydrogen SPR sensor is reached at a value of S = 7.99[nm] and below when it is fitted with a heterogeneous metallic nanolayer Ag-nd and N equal to 1000 [1/μm$^3$]. Since the Rmin value is 0.04 it can be used to detect hydrogen gas leaks early on.

## References

[1] K. Tomoda, N. Hoshi, J. Haruna, M. Cao, A.Yoshizaki, K. Hirata, IEEE Transactions on Industry Applications **50**(4), 2741 (2014); https://doi.org/10.1109/TIA.2013.2294994
[2] S. Ohta, Pharmacology & Therapeutics **144**(1), 1 **(**2014); https://doi.org/10.1016/j.pharmthera.2014.04.006
[3] G. Korotcenkov, Handbook of Gas Sensor Materials: Properties, Advantages and Shortcomings for Applications: Conventional Approaches, Integrated Analytical Systems, Springer New York, New York, (2013); https://doi.org/10.1007/978-1-4614-7165-3
[4] WP. Jakubik, M. Urbańczyk ,E. Maciak ,T. Pustelny, Acta Physica Polonica. A **116**(3), 315 **(**2009); https://doi.org/10.12693/APhysPolA.116.315
[5] K. Luongo, A. Sine, S. Bhansali, Sensors and Actuators B: Chemical **111-112**, 125 (2005); https://doi.org/10.1016/j.snb.2005.06.056

[6] B. Xie, L. Liu, X.Peng ,Y.Zhang,Q.Xu, The Journal of Physical Chemistry C **115**(32). 16161 **(**2011); https://doi.org/10.1021/jp2033752
[7] X. Bévenot, A.Trouillet , C.Veillas , H.Gagnire, M.Clément, Sensors and Actuators B: Chemical **67**(1-2), 57 (2000); https://doi.org/10.1016/S0925-4005(00)00407-X
[8] C. Ma, A. Wang, Optics Letters **35**(12), 2043 **(**2010); https://doi.org/10.1364/OL.35.002043
[9] N. Liu, ML. Tang, M. Hentschel, H. Giessen, AP. Alivisatos, Nature materials **10**(8), 631 **(**2011); https://doi.org/10.1038/nmat3029
[10] YH. Kim, MJ. Kim, BS. Rho, MS. Park, JH. Jang, BH. Lee, IEEE SENSORS JOURNAL **11**(6), 1423 **(**2011); https://doi.org/10.1109/JSEN.2010.2092423
[11] A. Tittl, P. Mai, R. Taubert, D. Dregely, N. Liu, H. Giessen, Nano Letters **11**(10), 4366 **(**2012); https://doi.org/10.1021/nl202489g
[12] K. Lin, Y. Lu, J. Chen, R. Zheng, P. Wang, H. Ming, Optics Express **16**(23), 18599 **(**2008); https://doi.org/10.1364/OE.16.018599
[13] F. Farahi, PA. Leilabady, JDC. Jones, DA. Jackson, Journal of Physics E: Scientific Instruments **20**(4), 432 (1987); https://doi.org/10.1088/0022-3735/20/4/018
[14] W. McKeehan, Physical Review **3**(21), 334 **(**1923); https://doi.org/10.1103/PhysRev.21.334
[15] M. Mitsushio, S. Higashi, M. Higo, Sensors and Actuators A: Physical **111**(2-4), 252 (2004). https://doi.org/10.1016/j.sna.2003.11.029
[16] J. Homola, Sensors and Actuators B: Chemical **29**(1-3), 401 (1995); https://doi.org/10.1016/0925-4005(95)01714-3
[17] D. Sil, KD. Gilroy, A. Niaux, A. Boulesbaa, S. Neretina, E. Borguet, ACS Nano **8**(8), 7755 **(**2014); https://doi.org/10.1021/nn500765t
[18] K.Takahashi, A. Hosoki, M. Nishiyama, H. lgawa, K. Watanabe, Photonic Instrumentation Engineering III 9754 (1), 188 (2016); https://doi.10/1117/12.2210826
[19] R. Jiang, F. Qin, Q. Ruan, J. wang, C. Jin, Advanced Functional Materials **24**(46), 7328 **(**2014); https://doi.org/10.1002/adfm.201402091
[20] S. Abdelali, S. Chouaib, Materials Today: Proceedings **31**(S1), S24-S27(2020); https://doi.org/10.1016/j.matpr.2020.05.278
[21] S. Abdelali, S. Chouaib, Journal of Optoelectronic and Biomedical Materials **12** (3), 73-79(2020).
[22] S. Abdelali, S. Chouaib, U.P.B. Sci. Bull., Series C: Electrical Engineering and Computer **83** (2), 73-79 (2021).
[23] MdB. Hossain, IM. Mehedi, M. Moznuzzaman, LF. Abdulrazak, MA. Hossain, Results in Physics **15**, 102719(2019); https://doi.org/10.1016/j.rinp.2019.102719
[24] C. Caucheteur, V. Voisin, J. Albert, Optics Express **23**(3), 2918 **(**2015) ; https://doi.org/10.1364/OE.23.002918
[25] Maheswari, V. Ravi, KB. Rajesh, Digest Journal of Nanomaterials & Biostructures **18**(1), 221 **(**2023) ; https://doi.org/10.15251/DJNB.2023.181.221
[26] D. Roy, Applied Spectroscopy **55**(8). 1046 **(**2001); https://doi.org/10.1366/0003702011952947
[27] MV. Klein, TE. Furtak, Optik. Springer Berlin Heidelberg, Berlin, Heidelberg, (1988); https://doi.org/10.1007/987-3-642-73409-0
[28] J. Singh, Optical properties of condensed matter and applications. John Wiley, Chichester, England ; Hoboken, NJ, 434 (2006).
[29] M. Bass, Handbook of optics, McGraw-Hill, 2nd ed, New York, 4(1995).
[30] A.Vial, T. Laroche , Journal of Physics D: Applied Physics **40**(22), 7152 (2007); https://doi.org/10.1088/0022-3727/40/22/043
[31] B. Sareni, L. Krähenbühl, A. Beroual, C. Brosseau, Journal of Applied Physics **81**(5), 2375 (1997); https://doi.org/10.1063/1.364276
[32] B. Sareni, L. Krähenbühl, A. Beroual, C. Brosseau, Journal of Applied Physics **80**(3), 1688 (1996); https://doi.org/10.1063/1.362969
[33] AK.Pathak, S. Verma, N. Sakda, C. Viphavakit, R. Chitaree, BMA. Rahman, Photonics **10**(2), 122(2023); https://doi.org/10.3390/photonics10020122
[34] K. Chen, D. Yuan, Y. Zhao, Optics & Laser Technology **137**, 106808 (2021); https://doi.org/10.1016/j.optlastec.2020.106808

[35] WE.Vargas, N. Clark, F. Muñoz-Rojas, DE. Azofeifa, GA. Niklasson, Physica Scripta **94**(5), 055101 (2019); https://doi.org/10.1088/1402-4896/ab07ee
[36] WE.Vargas, Applied Optics **56** (3), 6496 (2017); https://doi.org/10.1364/AO.56.006496
[37] P. Maheswari, S. Subanya, V.Ravi, B. Rajesh, J. Rajan, J. Zbigniew, Plasmonics **1** (17), 213(2022); https://doi.org/10.1007/s11468-021-01507-5